Study of Synthetic Clay Minerals. V.[1)] Lamellar Fraipontite–Silica Composite as a New Adsorbent

Noriyuki Takahashi,* Masanori Tanaka, Teiji Satoh, and Tadashi Endo†

Mizusawa Industrial Chemicals, Ltd., Nakajo-machi, Niigata 959-26

†Department of Molecular Chemistry and Engineering, Faculty of Engineering, Tohoku University, Aramaki, Aoba, Sendai 980

(Received September 2, 1996)

A novel porous adsorbent was prepared by adding an aqueous solution having Zn, Al, and Si components into a suspension of silica hydrogel at 40 °C. According to the results of XRD, NMR, TEM etc., the adsorbent was identified as being a new composite consisting of lamellar fraipontite and silica. The layer structure of the resulting fraipontite was not stratified three-dimensionally. NMR data also verified that the structural framework consisted of a single ZnO_6 octahedral sheet with Al^{oct} and a single SiO_4 tetrahedral sheet with Al^{tet}, which bonded with silica. The formation process of this porous adsorbent, incorporated by silica particles, was systematically examined in some detail.

Many inorganic adsorbents are made from some clays, such as Fuller's earth, halloysite and allophane.[2)] Fuller's earth has been prepared in industry as a refining agent for bleaching fats and oils in the United Kingdom since the mid-nineteenth century.[3)] In Japan, activated bleaching earth[4)] has been produced by a chemical treatment of the Japanese acid clay,[5)] one of Fuller's earth, and has then been used as a refining agent for fats and oils,[6)] or mineral oils.[7)] The adsorbent is sufficiently available for use as a color developer of pressure-sensitive copying paper,[8)] and a considerable quantity is exported to Europe.

A 2 : 1-type clay mineral, which is mainly contained in Fuller's earth, consists of three sheets in a layered framework. One octahedral sheet is arranged inward, like a sandwich between two tetrahedral sheets. Consequently, the electrostatic effect of a cation constituting an octahedral sheet is slightly on the intersurface of a layer, which brings out the adsorption characteristics. On the other hand, a 1 : 1-type clay mineral is expected to show interesting adsorption characteristics, because the layer structure consists of both tetrahedral and octahedral sheets having different properties from electric and optical viewpoints.

Natural clays and related materials usually contain Mg and Al ions as cations occupying the octahedral sheet. Such cations are replaced by Fe, Mn, Cr, Co, Ni, Zn, and Cu ions with a few different ionic radii. Zinc oxide is colorless among these metal oxides.

Recently, we have reported on an artificial fraipontite,[9)] a Zn-containing species of a serpentine sub-group in 1 : 1-type clay minerals; its formula was $([Zn_{6-x}Al_x][Si_{4-x}Al_x]O_{10}(OH)_8)$. The fraipontite was expected to have some potential to arbitrarily control the adsorbent properties. The present paper demonstrated the synthesis of a new porous adsorbent comprising lamellar fraipontite and silica. In addition, the role of silica gel is discussed in terms of the stratification of the fraipontite unit layer from keeping a high surface area.

Experimental

Synthesis of the Typical LFS. Zn–Al–Cl system acidic aqueous solution (5.4 dm^3 (Zn: 9.6 mol, Al: 3.6 mol)) and sodium silicate alkaline aqueous solution (5.4 dm^3 (Si: 3.6 mol)) were added simultaneously for 70 min into 13 kg of a 4 wt% silica hydrogel suspension (Si: 8.4 mol) under stirring, while being kept at 40 °C, and then aged for 30 min. After the slurry was filtered, the pH of the filtrate was adjusted to be 7.0. The remaining salt in the cake was sufficiently washed out with water, then dried at 130 °C to yield 1.68 kg of product **1**, which was called LFS, referring to Lamellar Fraipontite–Silica. Product **1** means the product of Run 1. Products **2** to **19** were obtained by a procedure similar to that used for Run 1 (Tables 1 and 2).

Analysis. The specific gravity ρ of the products were determined using a Micromeritics Heliun Pycnometer 1302-02. The specific surface area (S) and the pore volume (V) of the products were determined by a nitrogen-adsorption method using a Carlo

Table 1. Characteristics of the Products Depending on the Matrix Silica Content at the Preparation of LFS

Run No.	Matrix silica Content	Product	
		S	ρ_b[a)]
	wt%	$m^2\ g^{-1}$	$g\ cm^{-3}$
1	4	300	0.20
2	3	310	0.21
3	1.2	340	0.30
4	0.6	290	0.38
5	0.3	320	0.63
6	0	170	0.63

a) ρ_b: Bulk density.

Table 2. Surface Characteristics of the Products Depending on the Atomic Fraction of Reactant Components

Run No.	Atomic fraction of reactant Zn %	Al %	Si %	Si_{mat}[a] %	Product S $m^2\,g^{-1}$	V $cm^3\,g^{-1}$	Phase
1	38.1	14.3	14.3	33.3	300	0.49	LFS
7	14.3	14.3	7.1	64.3	480	0.67	LFS
8	24.1	13.8	13.8	48.3	420	0.62	LFS
9	25.8	24.0	17.2	33.0	378	0.55	LFS
10	31.8	14.0	21.2	33.0	306	0.58	LFS
11	32.2	24.0	10.8	33.0	340	0.45	LFS
12	37.8	4.0	25.2	33.0	248	0.46	LFS
13	38.7	24.0	4.3	33.0	269	0.38	LDH[b]+LFS
14	39.8	14.0	13.2	33.0	286	0.55	LFS
15	42.9	14.3	14.3	28.6	280	0.39	Unknown+LFS
16	47.2	4.0	15.8	33.0	241	0.44	LFS+LDH
17	47.7	14.0	5.3	33.0	245	0.36	LDH+LFS
18	53.3	13.3	0.0	33.3	220	0.35	LDH+LFS
19	56.7	4.0	6.3	33.0	171	0.30	LDH+LFS

a) Si_{mat}: silicon in matrix silica. b) LDH: layered double hydroxide.

Erba Sorptomatic Series 1800. The surface areas were calculated using the BET equation. The X-ray diffraction (XRD) patterns of the products were obtained by a Rigaku Denki Geiger Flex using Ni-filtered Cu $K\alpha$ radiation at a scanning speed of $2\theta/2\,^\circ\,min^{-1}$. A transmission electron-microscopic observation was performed using a Hitachi H-7100 electron microscope. ^{29}Si and ^{27}Al MAS NMR spectra of samples were measured using a JEOL GX-270 FT-NMR spectrometer at 53.6 and 70.4 MHz, and the chemical shifts were referenced to tetramethylsilane (TMS) and $[Al(OH_2)_6]^{3+}$, respectively. The measurements were carried out under the conditions of high-power dipolar decoupling (DD) and cross-polarization (CP). The pulse widths were 6.0 μs and 6.2 μs; the repetition times were 7.0 s (^{29}Si/DD), 4.0 s (^{29}Si/CP) and 5.0 s (^{27}Al/DD); and the contact time was 3 ms (^{29}Si/CP), respectively. The IR spectra were measured by a Nihon-Bunko A-302 Spectrometer using the KBr method. A differential thermal analysis (DTA) and thermogravimetry (TG) were carried out using a Rigaku Denki TG-DTA/S apparatus. All of the DTA and TG analyses were carried out under the conditions of a constant heating rate of 10 °C min^{-1} and an air flow rate of 50 $cm^3\,min^{-1}$.

Results and Discussion

Design for the LFS Synthesis. Table 1 summarizes the influence of the silica hydrogel content in a suspension of the reaction mixture upon the properties of the LFS products. The silica hydrogel, hereinafter called matrix silica, participated in the formation of a macropore, since the higher is the content of matrix silica, the smaller is the bulk density (ρ_b). The macropore increases the adsorption ability, since molecules easily diffuse into there. The presence of matrix silica contributed to the formation of a mesopore, because the specific surface area (S), correlated to a mesopoer, showed approximately constant high values over the content range of the matrix silica. A solid content of 3—4 wt% in a matrix silica suspension is therefore desirable to produce a new adsorbent having a large space capacity.

Table 2 shows the characteristics of products depending on the ratio of the constituents used in the LFS synthesis. Phases other than LFS also appeared in some cases. Layered double hydroxides ($Zn_{3-x}Al_x(OH)_6[Cl_y(CO_3)_{2z}]_{x/(y+2z)}\cdot nH_2O$)[10] were observed in products **13**, **16**—**18**, and **19**. Product **15** showed a weak basal reflection, whose spacing was 1.26 nm, and hardly shifted after an ethylene glycol treatment. This result means that the product was neither sauconite ($Na_xZn_3[Si_{4-x}Al_x]O_{10}(OH)_2$) nor zinc phyllosilicate ($Zn_3Si_4O_{10}(OH)_2$). It is expressed as an unknown phase in Table 2.

Figure 1 gives the Zn, Al, and Si compositions of the reaction mixtures which produced LFS. Either the Zn fraction was more than 40 mol% (Run 15—19) or the Si fraction was less than 5 mol%, though the Zn fraction was less than 40 mol% (Run 13); in such cases the total silica component was insufficient to form the tetrahedral sheet of fraipontite, even if a small amount of the silica component was supplied from matrix silica. An excess amount of Zn induced the formation of layered double hydroxides. Accordingly, there is suitable range of source composition to produce the LFS. With increasing the matrix silica component, even in this range, the X-ray powder diffraction intensity of the fraipontite component decreased, and the values of S and the pore volume (V) approached those of only matrix silica, for example Run 7 (Tables 2 and 3). Product **1**, containing 38.1 mol% of the Zn fraction will be examined hereinafter, because it produces an expectation of being able to exhibit the characteristics of fraipontite among these LFS.

Physical Characteristics of LFS. Figure 2 shows transmission electron micrographs of product **1** and silica gel. Silica gel consisted of spherical particles, which were linked three-dimensionally to each other, being approximately 10 nm diameter. Product **1** showed not only spherical silica

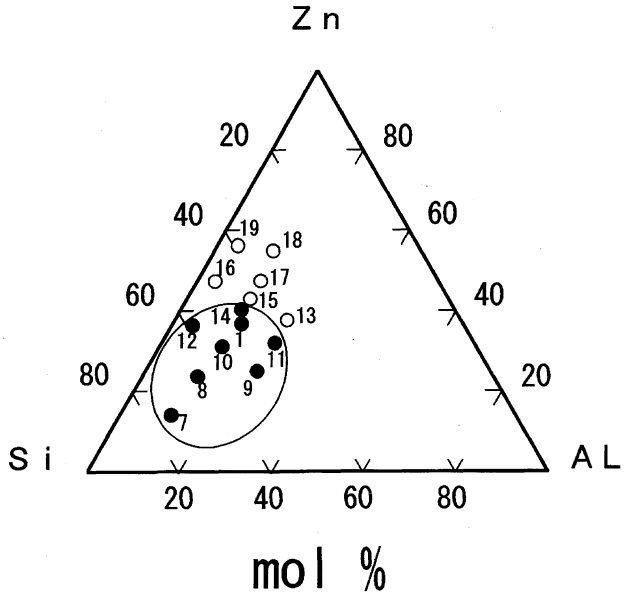

Fig. 1. Compositions of Zn, Al, and Si in the examined reaction mixtures. Inside of the circle is the compositional region producing LFS.

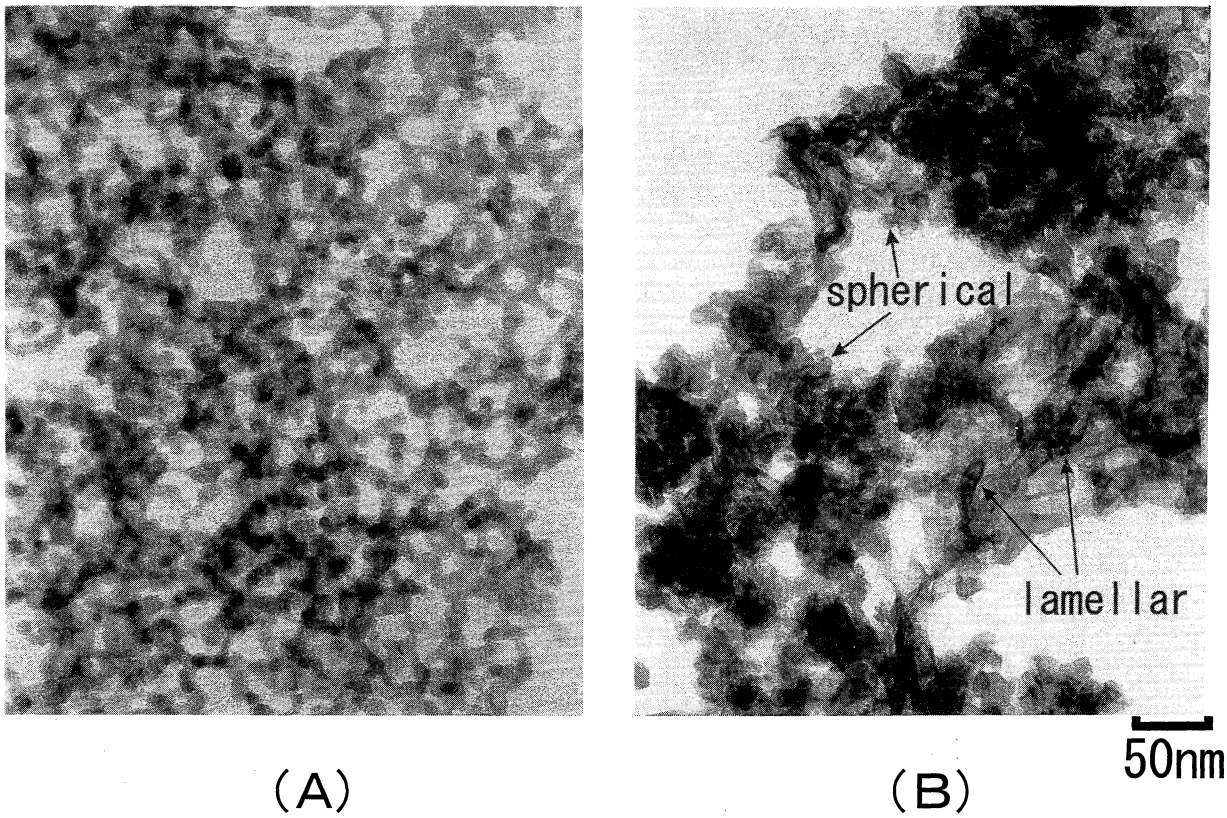

Fig. 2. Transmission electron micrographs of (A) matrix silica and (B) LFS.

Table 3. Characteristic of Product **1**, CPF and Silica

Sample	$S^{a)}$	$V^{b)}$	$\rho^{c)}$	$D_S{}^{d)}$
	$m^2\,g^{-1}$	$cm^3\,g^{-1}$	$g\,cm^{-3}$	nm
CPF	170	0.42	3.3	10.7
Product **1**	300	0.49	3.0	6.8
Silica gel	600	0.89	2.2	4.5

a) S: Specific surface area. b) V: Pore volume. c) ρ: Specific gravity. d) D_S: Specific surface diameter.

particles, but also random-shape lamellar crystallites, which became dispersed in the space among the silica particles. In other words, the matrix of silica gel prevented the lamellar crystallite from stacking to become a fraipontite crystal.

Table 3 shows some characteristics of fraipontite sythesized by the coprecipitation method[9] (hereinafter called CPF), product **1** and matrix silica. Product **1** had larger S and V values than those of CPF, and was thus porous. The specific surface diameter (D_S) was calculated using $D_S=6/(S\times\rho)$ based on the assumption that these particles were spherical; the value of product **1** was intermediate between that of CPF and the silica gel.

The nitrogen adsorption isotherms of product **1** and silica gel are shown in Fig. 3. Product **1** showed the BET-type isotherm accompanying hysteresis designated as H3 (type B) by IUPAC.[11] In other words, the pore was formed in the slit shape by platy particles. On the other hand, the silica gel showed a Langmuir-type isotherm. Micropore structure analyses were performed for these isotherms by the MP-method.[12] The silica gel had micropores, while product **1**

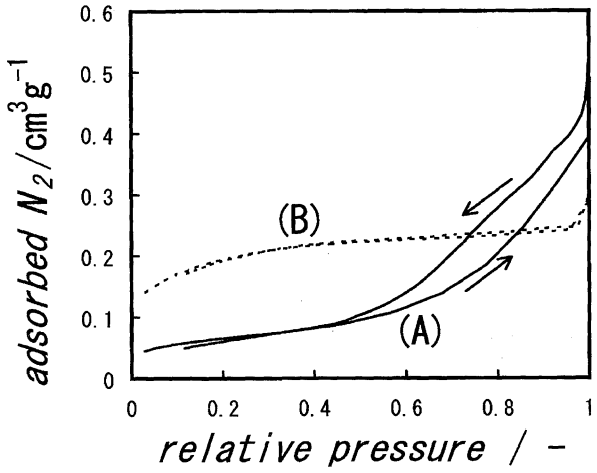

Fig. 3. Nitrogen adsorption isotherms of (A) LFS and (B) silica gel.

showed only a few such pores.

Structure of CPF and Silica Gel Figure 4B shows the X-ray powder diffraction profile of CPF; each peak was indexed as (001), (020), (130) or (060) diffractions based on a comparison with Fig. 4A.

Figure 5C shows the ^{29}Si NMR spectrum of CPF; the peak at -84.3 ppm was assigned to $Q^3(2Al)$[13] in the tetrahedral layer of fraipontite structure. Figure 5E shows two peaks of ^{27}Al. One peak at 64.7 ppm was assigned to Al in a tetrahedral sheet (Al^{tet}); the other peak at 11.3 ppm was assigned to Al in a octahedral sheet (Al^{oct}) of fraipontite.[13] The Al^{tet} peak showed a 2.1 ppm high-field shift from that of

fraipontite, suggesting that the mean Al–O–Si bond angle of CPF became wider than that of fraipontite.[14] The full widths at half maximum were 17 and 10 ppm, respectively.

The silica gel used as matrix component of LFS showed the peaks of Q^2 at −91.7, Q^3 at −101.4, and Q^4 at −110.2 ppm. Since the Q^3 peak was the strongest among them, ^1H certainly existed around Q^3. Accordingly, the silica gel consisted not only of a Q^4 unit in a three-dimensional silica structure, caused by the dehydration condensation of SiOH groups, but also of Q^3 and Q^2 units still bearing a hydroxyl group.

Structure of LFS. The X-ray powder diffraction pattern of product **1** in Fig. 4C shows (130) and (060) peaks of fraipontite, while it shows no reflection peak of (001). Therefore, product **1** formed only a fraipontite (*hk*) plane, namely a "lamellar fraipontite" structure. Both the matrix silica (Fig. 4D) and product **1** exhibited a halo-type figure at around $2\theta = 22°$, which revealed the coexistence of matrix silica in product **1**. The LFS consisted of fraipontite, which was disordered in the [001] direction, and matrix silica in a similar manner to the two-dimensional talc,[15] which was a mixture of talc disordering in the [001] direction with silica.

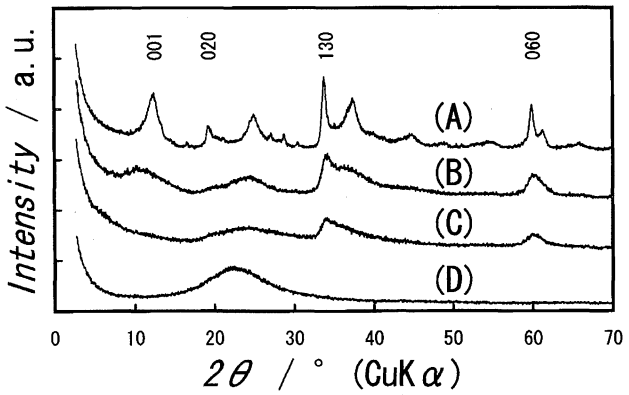

Fig. 4. X-Ray powder diffraction patterns of (A) fraipontite, (B) CPF, (C) LFS, and (D) silica gel.

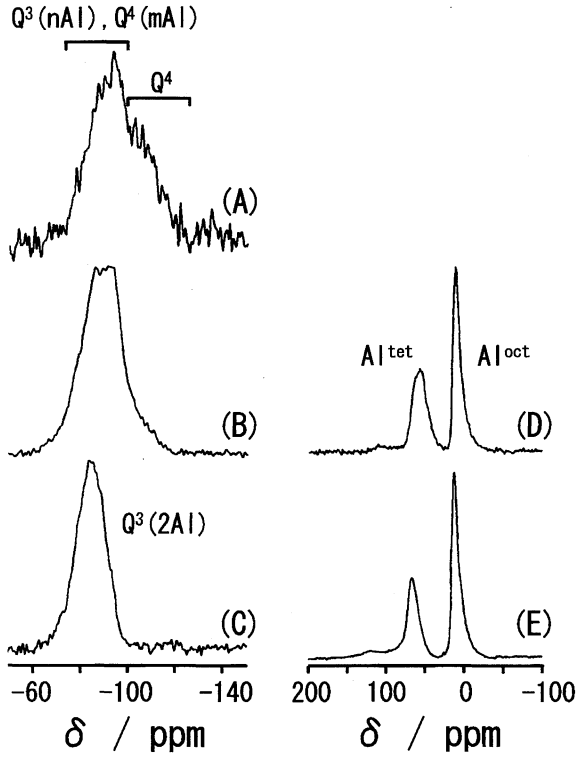

Fig. 5. MAS NMR spectrum of (A) ^{29}Si DD of LFS, (B) ^{29}Si CP of LFS, (C) ^{29}Si CP of CPF at 53.5 MHz and (D) ^{27}Al of LFS, (E) ^{27}Al of CPF at 70.3 MHz.

Figure 6 shows the IR spectrum of product **1** and fraipontite. The spectrum of product **1** showed the same peaks as did fraipontite at 790, 580 cm^{-1} and a shoulder at 900 cm^{-1}. Since the ν_{Si-O} mode of fraipontite[13] at 992 cm^{-1} was overlapped by the ν_{Si-O} mode of matrix silica at 1095 cm^{-1}, the peak apparently shifted to 1007 cm^{-1} and became wide.

Figure 5A shows the ^{29}Si/DD peaks of product **1** at −112——−103 assigned to Q^4 of tectosilisic acid,[16] and −98——−79 ppm assigned to Q^4 (*m*Al: $m = 2$ and 3) of tectosilicate[17] and Q^3 (*n*Al: $n = 0$, 1 and 2) of phyllosilicate.[18,19] The assignment to Q^4 (4Al) was neglected because product **1** had only 9 wt% of Al_2O_3 (Table 4). It is considered that Q^4 corresponds to matrix silica, and that both Q^4 (*m*Al) and Q^3 (*n*Al) correspond to the fraipontite structure. The ^{29}Si/CP spectrum was also measured in order to investigate the silicon having a short $Si-^1H$ distance. The enhanced peaks of product **1** in Fig. 5B were at −94.4——−86.7 ppm, which were assigned to Q^4 (2Al) of tectosilicate and Q^3 (*n*Al: $n = 0$ and 1) of phyllosilicate. The existence of Q^4 (2Al), in contrast to CPF, which showed only Q^3 (2Al), meant the formation of a new SiO–Al bond between an OH group of

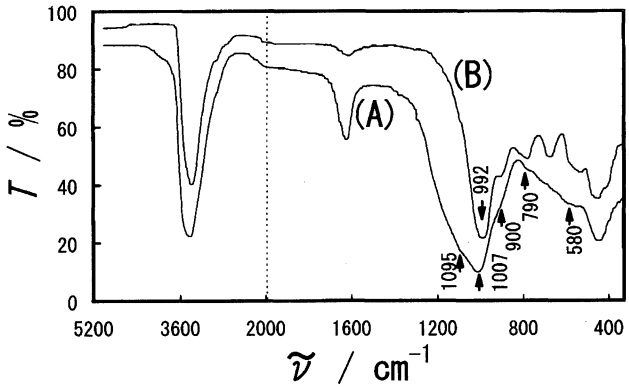

Fig. 6. IR spectrum of (A) LFS (B) fraipontite.

Table 4. Chemical Analysis of Product **1**

Component	wt%	mmol g^{-1}	Component	wt%	Molar ratio[b]
SiO_2	37.23	6.2	SiO_2	19.6	3.2
Al_2O_3	9.09	0.9	AlO_2	4.5	0.8
—			AlO	4.4	1.0
ZnO	40.77	5.0	ZnO	40.8	5.0
Ignition loss	12.23	—	OH	11.5	12.7
Na_2O	0.03	0.0	SiO_2	17.6	3.0
Cl^-	0.71	0.2	Cl^-	0.7	0.2
Total	99.35[a]	—	Total	99.1	—

a) Excluding the value of Cl. b) Based on $O_{10}(OH)_8$.

matrix silica and an Al of the fraipontite structure in product **1**. Product **1** had ^{1}H around Q^3 (1Al), exhibited by comparing Fig. 5A with B, while the silica gel of raw materials had it around Q^3. These results suggested that the surface SiOH group of Q^2 matrix silica reacted with the Al components to become Q^3 (nAl) in the fraipontite structure part and the surface SiOH group of Q^3 with Al to Q^4 (mAl) in a similar manner.

The ^{27}Al NMR of product **1** in Fig. 5D shows peaks at 55.3 and 10.6 ppm, assigned to Al in a tetrahedral sheet (Al^{tet}) and Al in an octahedral sheet (Al^{oct}) of the fraipontite structure part, respectively.[14,19] The full widths at half maximum were 22 and 11 ppm, respectively, and became wider than those of CPF. The peak of Al^{tet} shifted by about 9 ppm toward a high-field, which could not be explained by a change in the Al–O–Si bond angle. Therefore, the Al^{tet} should be assigned to $Al(OSi)_4$ in tectosilicate (q^4 (4Si)). The peak of Al^{oct} showed a chemical shift similar to that of CPF, suggesting that although the octahedral sheet was completed as a part of fraipontite, the tetrahedral sheet was distorted by bonding with matrix silica. The peak intensity ratio of Al^{tet} and Al^{oct} was 46 : 54.

Product **1** was a species of phyllosilicate based on the results of an X-ray diffraction analysis, although it showed Q^4 (mAl) and q^4 (4Si) in the NMR spectra. The atoms constituting this phyllosilicate crystal had to be located in their position with any variety of bonding distances and angles, suggesting that these atoms formed phyllosilicate on the long-range structure, while some atoms could be recognized to constitute tectosilicate on the short-range structure.

Chemical Composition of LFS. The chemical formula of product **1** on the basis of $O_{10}(OH)_8$ was evaluated based on both a chemical analysis (in Table 4) and ^{27}Al NMR, as well as on the assumption that the matrix silica made up for the lack of a silica component to form the fraipontite structure,

$$(Zn_{5.0}Al_{1.0})[Si_{3.2}Al_{0.8}]O_{10}(OH)_8(SiO_2)_{3.0}(H_2O)_{2.4}Cl_{0.2}.$$

The fraipontite-structure part and matrix-silica part maintain an electrostatic balance with each other in this formula.

Thermal Stability of LFS. The LFS was calcined for evaluating the heat-resistant property of the fraipontite part, consisting of LFS, and was examined by X-ray powder diffraction. The diffraction peak intensity of fraipontite decreased with increasing the calcining temperature. The diffraction peak of boehmite gel faintly appeared at 500 °C, indicating that the dissociation of the fraipontite structure commenced below this temperature. The highly crystallized fraipontite released lattice water at around 430 °C,[13] suggesting that the heat stability of the fraipontite structure part, comprising LFS, ought to be up to 400 °C.

Formation Process of LFS. Figure 7 shows the formation process of LFS schematically. The Zn, Al, and Si components of a salt solution formed fraipontite crystallites via aqua complexes, and then precipitated as an intermediate; this process was the same as in the CPF formation. One the other hand, polysilicate micro-particles were defloc-

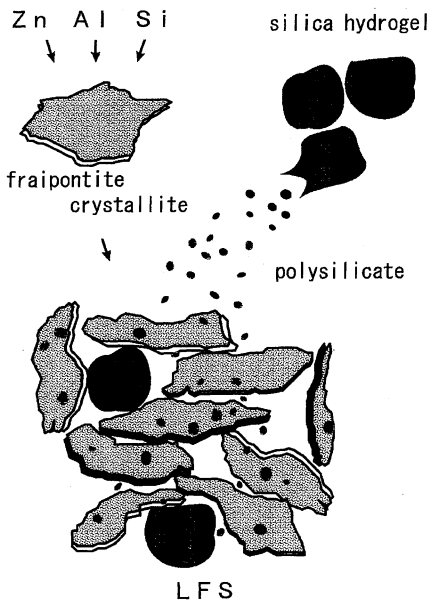

Fig. 7. Conceptual scheme of LFS formation process.

culated from the surface of silica hydrogel particles. After the fraipontite crystallites had condensed with the surface OH groups of silica hydrogel particles or polysilicate microparticles, the fraipontite crystallites could not stack regularly. The micropores existing in the silica gel had disappeared, and mesopores were newly formed by the fraipontite crystallite and silica particles. The LFS comprised Q^3 (nAl), Q^4 (mAl), and q^4 (4Si) units on the short-range structure, while it was a 1 : 1-type lamellar fraipontite bonded with silica hydrogel on the long-range structure.

Summary

The combination of fraipontite crystallites and silica gel produced a novel porous composite mainly consisted of mesopore with a large surface area. The composite was produced by precipitating fraipontite crystallites to the silica suspension and formed agglomeration, a so-called a house-of-cards structure, that was indicted by TEM. The agglomeration of fraipontite crystallites occurred during the course of the growing process, accompanied by bonding with silica gel, which was verified by NMR. The composite had the advantages of its production under atmospheric pressure, and a reduction of the Zn component by incorporating silica particles, as compared with the synthesis of fraipontite.

The authors acknowledge Dr. Shinichi Nakata of Chiyoda Co. for the MAS NMR measurement.

References

1) Part IV: N. Takahashi, M. Tanaka, T. Satoh, T. Endo, and M. Shimada, *Microporous Mater.*, in press.

2) H. Yanai, "Kyuchakuzai·Kyuchakusosa no Sekkei," Gihodo Shuppan, Tokyo (1983), p. 29.

3) R. E. Grim, "Applied Clay Mineralogy," McGraw-Hill, New York (1962), p. 320.

4) K. Yamamoto, "Kassei Hakudo," *Kogyo Kagaku Zasshi,*

Sup. No. 25 (1942).
5) K. Kobayashi, "Sansei Hakudo," Maruzen, Tokyo (1949), p. 1.
6) H. B. W. Patterson, "Bleaching and Purifying Fats and Oils," American Oil Chemists' Society, Illinois (1992), p. 85.
7) H. Kawakami, K. Teramoto, M. Soda, K. Hanano, and K. Abe, *Sekiyu Gakkai Shi*, **15**, 167 (1972).
8) Y. Tokunaga, *Kamipa Gikyo Shi*, **44**, 654 (1990).
9) N. Takahashi, M. Tanaka, and T. Satoh, *Nippon Kagaku Kaishi*, **1990**, 370.
10) S. Miyata, *Clays Clay Miner.*, **23**, 369 (1975).
11) S. J. Gregg and K. S. W. Sing, "Adsorption, Surface Area and Porosity," Academic Press, London (1982), p. 287.
12) R. Sh. Mikhail, S. Brunauer, and E. E. Bodor, *J. Colloid Interface Sci.*, **26**, 54 (1968).
13) N. Takahashi, M. Tanaka, and T. Satoh, *Nippon Kagaku Kaishi*, **1991**, 692.
14) E. Lippmaa, A. Samoson, and M. Mägi, *J. Am. Chem. Soc.*, **108**, 1730 (1986).
15) N. Takahash, M. Tanaka, T. Satoh, and T. Endo, *Bull. Chem. Soc. Jpn.*, **67**, 2463 (1994).
16) G. Engelhardt and D. Michel, "High-Resolution Solid-State NMR of Silicates and Zeolites," John Wiley and Sons, New York (1987), p. 170.
17) E. Lippmaa, M. Mägi, A. Samoson, G. Engelhardt, and A. -R. Grimmer, *J. Am. Chem. Soc.*, **102**, 4889 (1980).
18) N. C. M. Alma and G. R. Hays, *Anal. Chem.*, **56**, 729 (1984).
19) J. Sanz and J. M. Serratosa, *J. Am. Chem. Soc.*, **106**, 4790 (1984).